

Driving-Force Effects on the Rate of Long-Range Electron Transfer in Ruthenium-Modified Cytochrome *c*

Thomas J. Meade,[†] Harry B. Gray,^{*,†} and Jay R. Winkler^{*,‡}

Contribution No. 7842 from the Arthur Amos Noyes Laboratory, California Institute of Technology, Pasadena, California 91125, and Department of Chemistry, Brookhaven National Laboratory, Upton, New York 11973. Received September 9, 1988

Abstract: Two new Ru-modified, Zn-substituted derivatives of horse heart cytochrome *c* have been prepared, Ru₄L(histidine-33)-Zn-cyt *c* (a = NH₃; L = pyridine, isonicotinamide). Molecular mechanics modeling indicates that the 11.7 Å edge-to-edge separation between the redox centers is virtually identical with that reported for the Ru-pentaammine derivative. Rates of photoinduced charge separation and recombination in Ru₄L(His-33)-Zn-cyt *c* lie in the range of 2.0 × 10⁵–3.3 × 10⁶ s⁻¹ (22 °C). These kinetics, along with those already reported, provide a total of eight intramolecular electron-transfer reactions that have been measured in Ru-M-cyt *c* (M = Fe, Zn) at driving forces (–Δ*G*^o) ranging from 0.18 to 1.05 eV. The variation of the rate with driving force is in general agreement with the semiclassical theory of electron-transfer reactions. Fitting the Ru-Zn-cyt *c* charge-separation data yields a reorganization energy (λ) of 1.15 (5) eV and an electronic coupling matrix element (*H*_{AB}) of 0.13 (1) cm⁻¹. The charge-recombination data are fit with the parameters λ = 1.24 (5) eV and *H*_{AB} = 0.10 (1) cm⁻¹, and the Ru-Fe-cyt *c* electron-transfer rate can be described with λ = 1.2 eV and *H*_{AB} = 0.03 cm⁻¹.

The aim of our research into the electron-transfer reactions of metalloproteins is to identify and understand the factors that control the rates of these processes.¹ Semiclassical² and quantum mechanical³ theories have provided the following simple expression for the rate of nonadiabatic electron transfer between two centers held at fixed distance and orientation:

$$k_{ET} = \nu_N \kappa_E \kappa_N \quad (1)$$

In eq 1 ν_N corresponds to the frequency of motion along the reaction coordinate, κ_E describes the electronic coupling between donor and acceptor, and κ_N is a factor arising from the nuclear rearrangement that accompanies the electron transfer. This paper describes an examination of the dependence of k_{ET} on the driving force (–Δ*G*^o) for the reaction: a dependence that appears directly in κ_N ² and indirectly in κ_E .⁴

We have previously reported the rates of intramolecular electron transfer in the derivatized proteins Ru₄(His-33)-M-cytochrome *c* (a = NH₃; His = histidine; M = Fe,⁵ Zn⁶). This work demonstrated that the response of k_{ET} to changes in Δ*G*^o was consistent with the semiclassical theory of electron-transfer reactions. The range of Δ*G*^o spanned in those experiments, however, was too narrow to clearly define the parameters embedded in eq 1. In particular, the reorganization energy (λ) and the electronic coupling (κ_E) could only be confined to the ranges 1.2–1.85 eV and 10^{-4.6}–10^{-6.9}, respectively. Data from a broader range of driving forces are required to refine these parameters. Toward this end, Ru₄L(His-33) (L = pyridine (py), isonicotinamide (isn)) derivatives of Zn-substituted cytochrome *c* have been prepared. Molecular mechanics modeling of these tetraammine derivatives⁷ indicates that the conformations and edge-to-edge separations (11.7 Å) are nearly identical with those found in the pentaammine derivative (Figure 1). Rates of electron transfer have been measured by flash photolysis techniques to provide a total of eight intramolecular electron-transfer reactions spanning a 0.87-eV driving-force range.

Experimental Section

Materials. Aqueous solutions were prepared with deionized water prepared by passing house distilled water through a Millipore Q3 water purification system. Sodium phosphate buffers (NaP_i) were prepared from analytical grade reagents. Horse heart cytochrome *c* (Fe-cyt *c*, Type VI, was supplied by Sigma Chemical Co.

Preparations. Zn-substituted cytochrome *c* was prepared from commercial Fe-cyt *c* by a procedure described previously.⁶ Ru₄L(His-33)-Zn-cyt *c* (L = py, isn) samples were prepared by reacting Zn-cyt *c* with an excess of Ru₄L(OH₂)²⁺. The details of the preparation and

characterization of these derivatives will appear in a separate publication.⁸

Methods. Ru₄L(His-33)-Zn-cyt *c* samples were stored in the presence of an oxidant (Co(edta)⁻ or Co(phen)₃³⁺) to maintain the Ru center in the 3+ oxidation state. The excess Co(III) was removed just prior to kinetics measurements by FPLC or by gel filtration chromatography with Sephadex G25-150 resin. The buffer used in all kinetics experiments was μ = 0.1 M, pH = 7.0, NaP_i.

Intramolecular electron transfer in Ru-Zn-cyt *c* samples was measured by laser flash photolysis.⁶ Deoxygenated samples were held in 1-cm cuvettes and excited with pulses from the second harmonic of a mode-locked Nd:YAG laser (532 nm, 30 ps fwhm). Zn-porphyrin triplet state decay kinetics were monitored by transient absorption at 450 nm. Charge-recombination kinetics were measured by following the Zn-porphyrin radical cation signal at 675 nm.

Unless otherwise specified, protein samples were maintained at 4 °C. All manipulations of Zn-cyt *c* and its Ru-ammine derivatives were performed with the exclusion of room light.

Results and Discussion

Three distinct classes of electron-transfer reactions have been examined with Ru₄L(His-33)-M-cytochrome *c* (Ru-M-cyt *c*): those involving transfer between (i) Ru and Fe; (ii) Ru and the Zn-porphyrin triplet excited state (Zn*); and (iii) Ru and the Zn-porphyrin radical cation (Zn^{•+}). Rates of electron transfer between Ru and Fe were measured following bimolecular generation of a nonequilibrium population of Ru(II)-Fe(III)-cyt *c*,

(1) Mayo, S. L.; Ellis, W. R.; Crutchley, R. J.; Gray, H. B. *Science* **1986**, *233*, 948–952.

(2) (a) Marcus, R. A. *Annu. Rev. Phys. Chem.* **1964**, *15*, 155–196. (b) Marcus, R. A.; Sutin, N. *Biochim. Biophys. Acta* **1985**, *811*, 265–322.

(3) (a) Levich, V. G. In *Physical Chemistry: An Advanced Treatise*; Eyring, H., Henderson, D., Jost, W., Eds.; Academic Press: New York, 1970; Vol. 9B. (b) Kestner, N. R.; Logan, J.; Jortner, J. *J. Phys. Chem.* **1974**, *78*, 2148–2166. (c) Ulstrup, J.; Jortner, J. *J. Chem. Phys.* **1975**, *63*, 4358–4368. (d) Marcus, R. A.; Siders, P. *J. Phys. Chem.* **1982**, *86*, 622–630.

(4) (a) Beratan, D. N.; Hopfield, J. J. *J. Am. Chem. Soc.* **1984**, *106*, 1584–1594. (b) Beratan, D. N.; Onuchic, J. N.; Hopfield, J. J. *J. Chem. Phys.* **1985**, *83*, 5325–5329. (c) Beratan, D. N. *J. Am. Chem. Soc.* **1986**, *108*, 4321–4326.

(5) (a) Winkler, J. R.; Nocera, D. G.; Yocom, K. M.; Bordignon, E.; Gray, H. B. *J. Am. Chem. Soc.* **1982**, *104*, 5798–5800. (b) Nocera, D. G.; Winkler, J. R.; Yocom, K. M.; Bordignon, E.; Gray, H. B. *J. Am. Chem. Soc.* **1984**, *106*, 5145–5150.

(6) Elias, H.; Chou, M. H.; Winkler, J. R. *J. Am. Chem. Soc.* **1988**, *110*, 429–434.

(7) Calculations were performed with BIOGRAF/III version 1.40: BIOGRAF was designed and written by S. L. Mayo, B. D. Olafson, and W. A. Goddard III.

(8) Meade, T. J.; Gray, H. B.; Chang, I.-J.; Winkler, J. R., to be submitted for publication.

[†] Arthur Amos Noyes Laboratory.

[‡] Brookhaven National Laboratory.

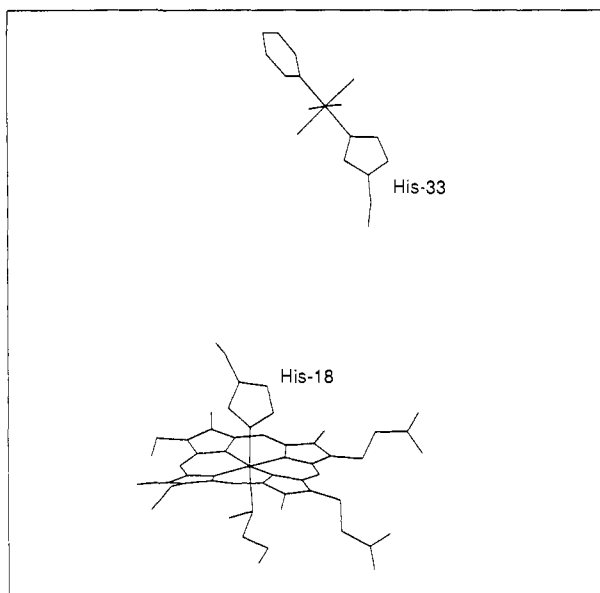


Figure 1. Minimum energy configuration of $\text{Ru}_4(\text{py})(\text{His-33})\text{-Fe-cyt } c$. Shortest distance from His-33 to His-18 is 11.7 Å.⁷

Table I. Rate Constants and Activation Parameters for the Ru-M-cyt *c* Intramolecular Electron-Transfer Reactions

| reaction ^a | $-\Delta G^\circ$, ^b eV | k_{obsd} , ^c s^{-1} | ΔH^\ddagger , ^d kcal mol^{-1} | ΔS^\ddagger , ^e eu | ref |
|---|--|---|--|--|----------|
| $\text{Ru}_4(\text{His-33})^{2+} \rightarrow \text{Fe(III)P}$ | 0.18 (1) | 3.0×10^1 | <2 | -46 | 5 |
| $\text{Ru}_4(\text{His-33})^{2+} \rightarrow \text{ZnP}^*$ | 0.36 (10) | 2.4×10^2 | 2.2 | -41 | 6 |
| $\text{Ru}_4(\text{Isn})(\text{His-33})^{2+} \rightarrow \text{ZnP}^{*+}$ | 0.66 (1) | 2.0×10^5 | <0.5 | -35 | <i>f</i> |
| $\text{ZnP}^* \rightarrow \text{Ru}_4(\text{His-33})^{3+}$ | 0.70 (1) | 7.7×10^5 | 1.7 | -27 | 6 |
| $\text{Ru}_4(\text{py})(\text{His-33})^{2+} \rightarrow \text{ZnP}^{*+}$ | 0.74 (1) | 3.5×10^5 | <0.5 | -34 | <i>f</i> |
| $\text{ZnP}^* \rightarrow \text{Ru}_4(\text{py})(\text{His-33})^{3+}$ | 0.97 (1) | 3.3×10^6 | 2.2 | -22 | <i>f</i> |
| $\text{Ru}_4(\text{His-33})^{2+} \rightarrow \text{ZnP}^{*+}$ | 1.01 (1) | 1.6×10^6 | | | 6 |
| $\text{ZnP}^* \rightarrow \text{Ru}_4(\text{Isn})(\text{His-33})^{3+}$ | 1.05 (1) | 2.9×10^6 | <0.5 | -30 | <i>f</i> |

^a FeP and ZnP refer to the metalloporphyrins in native-Fe and Zn-substituted cytochrome *c*, respectively. ^b Free-energy changes are derived from the following half-cell potentials (vs NHE, 25 °C): Fe(III/II)P, 0.26 V;⁵ $\text{ZnP}^{*+}/0$, 1.09 V;⁹ $\text{ZnP}^{*+}/*$, -0.62 V;⁹ $\text{ZnP}^{*+}/-$, 0.44 V;⁶ $\text{Ru}_4(\text{His})^{3+/2+}$, 0.08 V;⁵ $\text{Ru}_4(\text{py})(\text{His})^{3+/2+}$, 0.35 V;⁷ $\text{Ru}_4(\text{Isn})(\text{His})^{3+/2+}$, 0.43 V.⁷ ^c $T = 22$ °C. ^d ΔH^\ddagger is determined from the slope of a plot of $\ln k_{\text{obsd}}$ vs $(1/T)$. ^e ΔS^\ddagger is defined by $\Delta S^\ddagger = R \ln(A/\nu)$, where A is the Arrhenius preexponential factor and $\nu \approx 1 \times 10^{13} \text{ s}^{-1}$. ^f This work.

which relaxes via intramolecular electron transfer.⁵ Photoexcitation of the Zn-porphyrin in Ru-Zn-cyt *c* generates the strongly reducing triplet excited state ($E^\circ = -0.62 \text{ V vs NHE}^\circ$) which, in addition to its usual radiative and nonradiative pathways, decays via electron transfer to the Ru(III) center bound to His-33. In the case of $\text{Ru}_4(\text{His-33})\text{-Zn-cyt } c$, reductive quenching of ZnP^* has also been observed.⁶ The Ru(II) to ZnP^{*+} charge-recombination step follows the photoinduced charge separation. The rates of the eight intramolecular reactions measured thus far (Table I) vary from 30 to $3.3 \times 10^6 \text{ s}^{-1}$ over a range of free-energy changes from -0.18 to -1.05 eV. The dependences of the electron-transfer rates on temperature (5–40 °C) have been examined in seven of the eight systems and are in all cases rather mild ($\Delta H^\ddagger \leq 2 \text{ kcal mol}^{-1}$, Table I). Corresponding activation entropies are quite negative, which is consistent with weak electronic coupling between donors and acceptors in these long-range electron-transfer reactions.

The variation of rate with driving force is often described by the classical theory of electron-transfer reactions, which predicts

(9) This value is based on a 1.71-eV triplet-state energy. The estimated $\text{ZnP}^* c^{+}/0$ potential is in general agreement with those of five-coordinate Zn-porphyrins in nonaqueous solutions¹⁰ and with that determined for Zn-myoglobin.¹¹

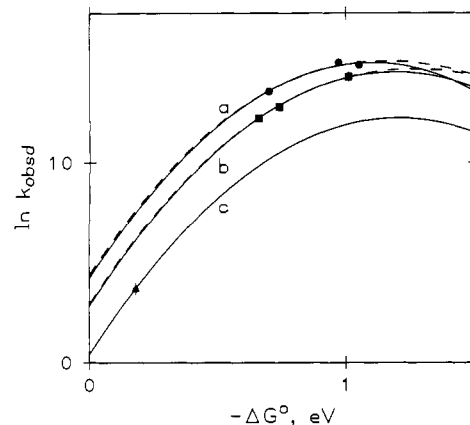


Figure 2. Plot of $\ln k_{\text{obsd}}$ vs $-\Delta G^\circ$ for the Ru-M-cyt *c* electron-transfer reactions: (●) ZnP^* to Ru(III) charge-separation reactions; (■) Ru(II) to ZnP^{*+} charge-recombination reactions; (▲) Ru(II) to Fe(III) electron transfer. Solid lines are best fits to eq 1 and 2 for the Ru-Zn-cyt *c* charge-separation reactions (a), charge-recombination reactions (b), and the Ru-Fe-cyt *c* electron-transfer reaction (c). Dashed lines are fit to a three-mode quantum-mechanical model (a and b).

that the nuclear factor, κ_N , will vary with ΔG° according to eq 2.² The reorganization energy λ is a quantity related to the

$$\kappa_N = \exp\{-(\Delta G^\circ + \lambda)^2/4\lambda RT\} \quad (2)$$

magnitude of nuclear reorganization (both of the reacting molecules and surrounding medium) that accompanies the electron transfer. In an ergoneutral ($\Delta G^\circ = 0$) electron-exchange reaction, the vertical energy difference between the product and reactant potential surfaces, at the equilibrium configuration of the reactants, is equal to λ . Given a series of electron-transfer reactions with constant κ_E and λ , but varying driving forces, eq 2 indicates that plots of $\ln k_{\text{ET}}$ vs ΔG° should be parabolic and that the maximum electron-transfer rate obtains when $-\Delta G^\circ = \lambda$. As ΔG° is varied, either by chemical modification of the redox sites or by studying different types of electron-transfer reactions, λ and κ_E are also likely to vary slightly. Within a given class of electron-transfer reactions, however, the fluctuations in λ and κ_E should be relatively minor. Fitting the Ru-Zn-cyt *c* charge-separation rates to eq 1 and 2 yields the parameters $\lambda = 1.10 \text{ eV}$ and $\nu_{\text{N}\kappa_E} = 3.3 \times 10^6 \text{ s}^{-1}$,¹² while the best fit to the charge-recombination data results with $\lambda = 1.19 \text{ eV}$ and $\nu_{\text{N}\kappa_E} = 2.0 \times 10^6 \text{ s}^{-1}$ (Figure 2). The similarity in λ for the two processes is consistent with the expectation that comparable nuclear reorganization accompanies the charge-separation and recombination reactions of Ru-Zn-cyt *c*.¹³

Configurational changes of both the inner coordination spheres of the metal centers (λ_{IN}) and the surrounding medium (λ_{OUT}) contribute to the total nuclear reorganization energy (λ) in Ru-M-cyt *c* ($\lambda = \lambda_{\text{IN}} + \lambda_{\text{OUT}}$). The inner-sphere contribution can be estimated from the structural changes that are known to accompany oxidation of Ru(II)-ammines and Zn-porphyrins. The Ru-N bond lengths generally change by less than 0.05 Å upon one-electron oxidation of Ru(II)-ammine complexes,¹⁵ and esti-

(10) Kadish, K. M.; Shiue, L. R.; Rhodes, R. K.; Bottomley, L. A. *Inorg. Chem.* **1981**, *20*, 1274–1277.

(11) Cowan, J. A.; Gray, H. B. *Inorg. Chem.*, in press.

(12) Since the reductive quenching of Zn-cyt *c* by $\text{Ru}_4(\text{His-33})^{2+}$ is a fundamentally different reaction with a very uncertain driving force, it will not be considered along with the other Ru-Zn-cyt *c* reactions.

(13) Kakitani and Mataga have discussed the contribution of the coordinated-solvent mode (C mode) to the total outer-sphere reorganization energy in charge-separation, charge-recombination, and charge-shift reactions.¹⁴ When one reactant is uncharged, the C mode reorganization energy need not be the same for these three processes. The magnitude of this effect, however, is diminished when both electron donor and acceptor are charged. The similarity in the values of λ found for the Ru-Zn-cyt *c* charge-separation and recombination reactions suggests that differences in C mode force constants are not important considerations in these particular reactions.

(14) Kakitani, T.; Mataga, N. *J. Phys. Chem.* **1987**, *91*, 6277–6285.

mates of the inner-sphere reorganization energies are on the order of 0.05 eV.¹⁶ An X-ray crystal structure of a Zn-porphyrin radical cation reveals fairly small changes in bond lengths and angles compared to the neutral precursor,¹⁷ and spectroscopic evidence indicates relatively minor distortions of the Zn-porphyrin upon excitation to the lowest lying triplet state.¹⁸ Hence, the contribution of the inner-sphere configurational changes about the Zn-porphyrin is not likely to be more than 0.15 eV, leading to an estimated upper limit of 0.2 eV for the total inner-sphere reorganization barrier in the Ru-M-cyt *c* intramolecular electron-transfer reactions.

The remaining contribution to λ in Ru-M-cyt *c* must arise from configurational changes of the solvent and polypeptide backbone of the protein (λ_{OUT}). Calculations of solvent reorganization energies typically treat the solvent as a dielectric continuum. The original Marcus model, which represents the reactants as two conducting spheres embedded in a dielectric continuum,² yields an estimate of 1.1 eV for the solvent reorganization energy in Ru-M-cyt *c*.²⁰ This model, however, is known to be inaccurate at small sphere-sphere separations.²¹ More sophisticated treatments describe the reorganization energy associated with transferring a single charge from one point to another within spherical or ellipsoidal cavities of low dielectric constant embedded in dielectric continua.²¹ Taking the Ru-M-cyt *c* system as a single sphere of 32-Å diameter leads to an estimate of 0.63 eV for the solvent reorganization energy.²² This value should be considered a lower limit to the solvent contribution to λ_{OUT} since roughly 45% of the volume in the minimum-enclosing 32-Å diameter sphere actually contains solvent, not a low dielectric medium. Neither solvent model accounts for reorganization of the protein matrix in response to the charge transfer, and this factor would have to be included in order to accurately calculate λ_{OUT} .²³

It is clear from the foregoing analysis that λ_{OUT} is the dominant component in the total reorganization energy for the Ru-Zn-cyt *c* electron-transfer reactions. The same is likely to be true for the Ru-Fe-cyt *c* reaction since λ_{OUT} should be much the same as found for Ru-Zn-cyt *c*, and crystallographic evidence reveals only minor structural differences between ferri- and ferrocytochrome *c*.^{24,25} Taking $\lambda = 1.2$ eV, which is comparable to λ found for charge-recombination in Ru-Zn-cyt *c* (1.19 eV), we estimate that $\nu_{\text{NKE}} = 2.0 \times 10^5 \text{ s}^{-1}$ for the Ru-Fe-cyt *c* reaction (Figure 2). The limiting rate is smaller for Ru-Fe-cyt *c* than that estimated for the Zn-derivatives, which implies weaker electronic coupling

Table II. Electronic Coupling Matrix Elements and Donor-Acceptor Separations of Several Intramolecular Electron-Transfer Systems

| donor-acceptor complex | $H_{\text{AB}},^a$ cm ⁻¹ | $R_{\text{E}},^b$ Å | $R_{\text{B}},^c$ bonds | ref |
|---|--|--------------------------|----------------------------|----------|
| P-Q ^d | 30 | 5.5 | 5 | 35 |
| D-Sp-A ^e | 4.6 | 10.2 | 10 | 34 |
| Os(II)-Pro ₁ -Ru(III) ^f | 4.3 | 7.2 (12.2) ^g | 5 | 43 |
| Os(II)-Pro ₂ -Ru(III) ^f | 2.2 | 9.8 (14.8) ^g | 8 | 43 |
| Os(II)-Pro ₃ -Ru(III) ^f | 0.8 | 13.1 (18.1) ^g | 11 | 43 |
| Ru-Zn-cyt <i>c</i> ^{*h} | 0.13 (1) | 11.7 | 49 (13) ⁱ | <i>j</i> |
| Ru-Zn-cyt <i>c</i> ^{+k} | 0.10 (1) | 11.7 | 49 (13) ⁱ | <i>j</i> |
| Ru-Fe-cyt <i>c</i> ^l | 0.03 | 11.7 | 49 (13) ⁱ | <i>j</i> |
| <i>c/b</i> ₅ ^m | 0.04 | 8 | none | 38 |

^a Electronic coupling matrix element, see eq 3. ^b Direct edge-to-edge distance between donor and acceptor. ^c Number of bonds separating donor and acceptor. ^d Covalently linked porphyrin-quinone molecules. ^e Steroid-bridged anion radical donors with aromatic hydrocarbon acceptors. ^f Polyproline-bridged Os-Ru ammine complexes. ^g Number in parentheses is the reported center-to-center separation. ^h From a fit to the Ru-Zn-cyt *c* charge-separation data. ⁱ Number in parentheses is the through-bond distance when Pro-30 to His-18 hydrogen-bonded contact is included. ^j This work. ^k From a fit to the Ru-Zn-cyt *c* charge-recombination data. ^l Estimate for the Ru-Fe-cyt *c* reaction assuming $\lambda = 1.2$ eV. ^m Cytochrome *c*/cytochrome *b*₅ ion pair.

between the Fe-porphyrin and the Ru-ammines.

In the Marcus theory of electron-transfer reactions, the nuclear reorganization energy is treated classically. An obvious refinement to this model would treat the higher frequency vibrational modes quantum mechanically. The three-mode model described by Brunschwig and Sutin²⁶ lends itself well to the Ru-Zn-cyt *c* system. The two inner-sphere modes, Zn-porphyrin and Ru-ammine rearrangements, can be described by quantum mechanical harmonic oscillators, while the outer-sphere reorganization retains a classical description. This model has six adjustable parameters, which cannot be determined from the three Ru-Zn-cyt *c* charge-separation or recombination data points. Reasonable estimates for the frequencies and reorganization energies of the two quantum modes can be supplied (vide supra), however, leaving just the two parameters λ_{OUT} and ν_{NKE} .²⁷ The results of fits to Ru-Zn-cyt *c* charge-separation and recombination data are shown by the dashed lines in Figure 2; the optimized values of λ and ν_{NKE} are 1.19 eV and $4.4 \times 10^6 \text{ s}^{-1}$ for charge separation and 1.29 eV and $2.9 \times 10^6 \text{ s}^{-1}$ for charge recombination. In both cases, only a modest refinement of the classical result is realized because quantum corrections arising from nuclear tunneling are most important in the "inverted" driving-force region ($-\Delta G^\circ > \lambda$).

The dynamics of conformational motion have also been postulated to affect or even limit electron-transfer rates in metalloproteins.^{28,29} In this case the observed rate constants would not be described simply by eq 1 and 2, because these expressions do not take into account the energetics and interconversion dynamics of all accessible protein conformational states. One interpretation of the data illustrated in Figure 2 would be that the slight flattening at higher driving forces ($-\Delta G^\circ \geq 0.8$ eV) is not due to the approach of $-\Delta G^\circ$ to λ but rather results from k_{ET} surpassing the rate of protein conformational motion. This dynamical limit is analogous to the diffusion limit encountered in bimolecular reactions, which effectively masks the upper portion of a parabolic rate vs free-energy plot. A standard steady-state kinetic model can describe this behavior, but fits to the complete Ru-M-cyt *c* data set yield extremely large values of λ . Our present set of data provides no strong positive evidence that the leveling of k_{ET} at high driving forces arises from protein conformational dynamics, but a definitive conclusion must await further studies.

(26) Brunschwig, B. S.; Sutin, N. *Comments Inorg. Chem.* **1987**, *6*, 209-235.

(27) The parameters used in the fitting procedure were as follows: $\lambda_1 = 0.15$ eV, $\hbar\omega_1 = 1500 \text{ cm}^{-1}$; $\lambda_2 = 0.05$ eV, $\hbar\omega_2 = 400 \text{ cm}^{-1}$.

(28) Hoffman, B. M.; Ratner, M. A. *J. Am. Chem. Soc.* **1987**, *109*, 6237-6243.

(29) McLendon, G.; Pardue, K.; Bak, P. *J. Am. Chem. Soc.* **1987**, *109*, 7540-7541.

(15) Gress, M. E.; Creutz, C.; Quicksall, C. O. *Inorg. Chem.* **1981**, *20*, 1522-1528.

(16) (a) Brown, G. M.; Sutin, N. *J. Am. Chem. Soc.* **1979**, *101*, 883-892. (b) Siders, P.; Marcus, R. A. *J. Am. Chem. Soc.* **1981**, *103*, 741-747.

(17) (a) Collins, D. M.; Hoard, J. L. *J. Am. Chem. Soc.* **1970**, *92*, 3761-3771. (b) Spaulding, L. D.; Eller, P. G.; Bertrand, J. A.; Felton, R. H. *J. Am. Chem. Soc.* **1974**, *96*, 982-987.

(18) The low-temperature fluorescence and phosphorescence spectra of Zn-cyt *c* contain only a few sharp bands, rather than long vibronic progressions, indicating that the singlet and triplet excited states are not significantly distorted from the ground-state geometry (<0.15 eV).¹⁹

(19) (a) Vanderkooi, J. M.; Adar, F.; Erecinska, M. *Eur. J. Biochem.* **1976**, *64*, 381-387. (b) Koloczek, H.; Fidy, J.; Vanderkooi, J. M. *J. Chem. Phys.* **1987**, *87*, 4388-4394.

(20) The two spheres were assigned radii of 13 and 3 Å and were taken to be in contact.

(21) Brunschwig, B. S.; Ehrenson, S.; Sutin, N. *J. Phys. Chem.* **1986**, *90*, 3657-3668.

(22) A 32-Å diameter sphere is the minimum volume sphere that will completely enclose two contacting 26-Å and 6-Å spheres (Zn-cyt *c* and Ru_a(His-33)³⁺, respectively). The following parameters were used in the calculation of λ_{OUT} using the single-sphere model: sphere radius, 16 Å; distance from center of sphere to point charges, 7.5 Å (Zn, Fe), 13 Å (Ru); center-to-center separation of the point charges, 18 Å; dielectric constant of the sphere, 1.8; bulk dielectric constant of the solvent, 78.54; optical dielectric constant of the solvent, 1.78.

(23) A calculation of the protein reorganization energy in the self-exchange reaction of native cytochrome *c* yields a value of 0.3 eV, suggesting a contribution on the order of 0.15 eV from protein dielectric relaxation to λ_{OUT} in Ru-M-cyt *c*.²⁴

(24) Churg, A. K.; Weiss, R. M.; Warshel, A.; Takano T. *J. Phys. Chem.* **1983**, *87*, 1683-1694.

(25) Tsunehiro, T.; Trus, B. L.; Mandel, N.; Mandel, G.; Kallai, O. B.; Swanson, R.; Dickerson, R. E. *J. Biol. Chem.* **1977**, *252*, 776-785.

The analysis of the Ru-M-cyt *c* driving-force data indicates a 1.2 (1)-eV reorganization energy³⁰ and maximum rate constants of $3.9(6) \times 10^6$, $2.5(5) \times 10^6$, and $2.0 \times 10^5 \text{ s}^{-1}$ for the Ru-Zn-cyt *c* charge-separation reactions, Ru-Zn-cyt *c* charge-recombination reactions, and Ru-Fe-cyt *c* reaction, respectively. In the nonadiabatic limit (i.e., $\kappa_E \ll 1$) the limiting electron-transfer rate is given by eq 3.² The term H_{AB} in eq 3 is the donor-acceptor

$$\nu_{N\kappa_E} = 2\pi H_{AB}^2 / \hbar (4\pi\lambda RT)^{1/2} \quad (3)$$

electronic coupling matrix element. Given the above values for $\nu_{N\kappa_E}$, we can estimate that $H_{AB} = 0.13$ (1) cm^{-1} for the charge-separation reactions, $H_{AB} = 0.10$ (1) cm^{-1} for charge-recombination processes, and $H_{AB} = 0.03 \text{ cm}^{-1}$ for Ru-Fe-cyt *c*.

It is interesting to compare the electronic coupling in Ru-M-cyt *c* to other systems in which H_{AB} can be evaluated from driving-force or temperature-dependence studies. This comparison is set out in Table II. The most obvious parameter upon which H_{AB} should depend is the donor-acceptor separation. Theory predicts that the decay of H_{AB} with distance should be exponential,^{2,4} but the appropriate distance measurement remains unclear.³⁴ Since the direct edge-to-edge separations and the through-bond distances tend to track one another in the synthetic donor-acceptor complexes,³⁴⁻³⁶ both measurements adequately describe the distance dependence of H_{AB} . In the two protein systems (Ru-M-cyt *c* and *c/b₅*³⁷), however, a through-bond pathway either does not exist or is considerably longer than the direct pathway. Table II clearly demonstrates that, in terms of direct separation, the electronic coupling in the protein systems is substantially smaller than that in synthetic complexes with comparable separations. The temptation is to suggest that through-bond pathways are operative in the long-distance electron-transfer reactions. The electronic coupling in Ru-M-cyt *c*, however, appears to be too large for the 49-bond path from His-33 to His-18 (the axial ligand of the metal in the porphyrin), and, in the *c/b₅* system, no covalent-bond pathway exists at all. Furthermore, a study of the distance dependence of intramolecular electron transfer in a series of Ru-modified Zn-substituted myoglobins has revealed that the rate does not correlate with the through-peptide distance.³⁹ If the restriction to covalent bonds is relaxed and hydrogen bonds or ionic contacts are included,⁴⁰ then a reasonable through-bond path

can be found for the Ru-M-cyt *c* system as well.^{41,42}

It would be premature to conclude that through-bond pathways (including hydrogen-bonded contacts) are the appropriate distances to examine when considering the magnitude of H_{AB} . Factors other than donor-acceptor separation contribute to this matrix element: factors that can easily obfuscate the analysis. The absolute redox level of the transferring electron is an important variable believed to affect the electronic coupling between donors and acceptors.⁴ The distance-normalized coupling in the polyproline-bridged metal dimers,⁴³ for example, is consistently smaller than in the P-Q and D⁻-Sp-A systems. At first glance this might suggest that the electronic coupling through polypeptide bridges is less efficient than through saturated hydrocarbon linkages. Closer examination, however, reveals that the energies of donor states in P-Q and D⁻-Sp-A are substantially higher than that of $\text{Os}a_5(\text{isn})^{2+}$; in addition, the radial extension of donor wave functions onto the bridge is likely to be somewhat greater in the excited porphyrins and aromatic radical anions than in the Os(II)-ammine complexes. Either effect alone, or the two in combination, could account for the minor differences in coupling among the three synthetic systems. In this light, it is somewhat surprising that the Ru-Zn-cyt *c* charge-separation and recombination rates agree as well as they do. Clearly, comparisons of H_{AB} in different donor-acceptor complexes must be made with great caution, owing to the complex dependence of this matrix element on a diverse set of parameters.

Summary

Measurements of the rates of electron transfer as a function of driving force have permitted some refinement of the values of the reorganization energy and electronic coupling in Ru-Zn-cyt *c*: $\lambda = 1.15$ (5) eV and $H_{AB} = 0.13$ (1) cm^{-1} for the photoinduced charge-separation reactions; $\lambda = 1.24$ (5) and $H_{AB} = 0.10$ (1) cm^{-1} for the recombination processes. Taking $\lambda = 1.2$ eV leads to an estimate of $H_{AB} = 0.03 \text{ cm}^{-1}$ for the Ru-Fe-cyt *c* reaction. For all three cases, the maximum electron-transfer rate constant is smaller than expected when compared to synthetic donor-acceptor complexes with comparable through-space separations. It is not possible, however, to attribute this difference to the activity of through-bond electron-transfer pathways in Ru-M-cyt *c* because of the possible variation of the electronic coupling matrix element with, among other factors, the absolute redox level of the transferring electron. Resolution of this point must await further studies of the distance dependence of electron transfer in protein systems with widely varying donor state energies.

Acknowledgment. We thank Dr. Norman Sutin for helpful discussions and Dr. Bruce Brunshwig for assistance with the calculations of λ_{OUT} . Research performed at Brookhaven National Laboratory was carried out under contract DE-AC02-76CH00016 with the U.S. Department of Energy and supported by its Division of Chemical Sciences, Office of Basic Energy Sciences. Research at the California Institute of Technology was supported by the National Science Foundation (CHE85-09637 and CHE85-18793).

(30) This value is smaller than the reorganization energies estimated for analogous Ru-M-myoglobin derivatives: five reactions, $\lambda = 1.90$ – 2.45 eV;³¹ six excited-state reactions, $\lambda = 1.3$ (3) eV;³² ten reactions, $\lambda = 1.6$ (1) eV.³³

(31) Karas, J. L.; Lieber, C. M.; Gray, H. B. *J. Am. Chem. Soc.* **1988**, *110*, 599–600.

(32) Cowan, J. A.; Upmacis, R. K.; Beratan, D. N.; Onuchic, J. N.; Gray, H. B. *Annals N.Y. Acad. Sci.* **1988**, *550*, 68–84.

(33) Karas, J. L. Ph.D. Thesis, California Institute of Technology, Pasadena, CA, 1989.

(34) (a) Miller, J. R.; Calcaterra, L. T.; Closs, G. L. *J. Am. Chem. Soc.* **1984**, *106*, 3047–3049. (b) Closs, G. L.; Calcaterra, L. T.; Green, N. J.; Penfield, K. W.; Miller, J. R. *J. Phys. Chem.* **1986**, *90*, 3673–3683. (c) Closs, G. L.; Miller, J. R. *Science* **1988**, *240*, 440–447.

(35) Wasielewski, M. R.; Niemczyk, M. P.; Svec, W. A.; Pewitt, E. B. *J. Am. Chem. Soc.* **1985**, *107*, 1080–1082.

(36) Oevering, H.; Paddon-Row, M. N.; Heppener, M.; Oliver, A. M.; Cotsaris, E.; Verhoeven, J. W.; Hush, N. S. *J. Am. Chem. Soc.* **1987**, *109*, 3258–3269.

(37) *c/b₅* is the one-to-one ion pair formed between cytochrome *c* and cytochrome *b₅*.³⁸

(38) McLendon, G.; Miller, J. R. *J. Am. Chem. Soc.* **1985**, *107*, 7811–7816.

(39) Axup, A. W.; Albin, M.; Mayo, S. L.; Crutchley, R. J.; Gray, H. B. *J. Am. Chem. Soc.* **1988**, *110*, 435–439.

(40) Beratan, D. N.; Onuchic, J. N.; Hopfield, J. J. *J. Chem. Phys.* **1987**, *86*, 4488–4498.

(41) A hydrogen-bonded contact between the carboxyl oxygen of Pro-30 and the imidazole nitrogen of His-18 gives a 13-bond separation.²⁵

(42) The discrepancies between the synthetic and protein systems could also be due to electron-transfer rates that are limited by protein conformational motion.

(43) Isied, S. S.; Vassilian, A.; Wishart, J. W.; Creutz, C.; Schwarz, H. A.; Sutin, N. *J. Am. Chem. Soc.* **1988**, *110*, 635–637.